

Structure and Energy Level Alignment of Tetramethyl Benzenediamine on Au(111)

M. Kamenetska,[†] M. Dell'Angela,^{‡,§,⊥} J.R. Widawsky,[†] G. Kladnik,^{‡,||} A. Verdini,[‡] A. Cossaro,[‡] D. Cvetko,^{‡,||} A. Morgante,^{*,‡,⊥} and L. Venkataraman^{*,†}

[†]Department of Applied Physics and Applied Mathematics, Columbia University

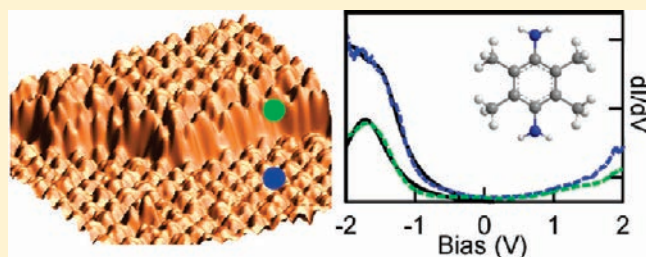
[‡]CNR IOM Laboratorio Nazionale TASC, Trieste, Italy

[§]Institut für Experimentalphysik, University of Hamburg, Hamburg, Germany

^{||}Department of Physics, University of Ljubljana, Ljubljana, Slovenia

[⊥]Department of Physics, University of Trieste, Trieste, Italy

ABSTRACT: We investigate the binding and energy level alignment of 2,3,5,6-tetramethyl-1,4-benzenediamine (TMBDA) on Au(111) through a combination of helium atom scattering (HAS), X-ray photoemission (XPS), and scanning tunneling microscopy (STM). We show that TMBDA binds to step edges and to flat Au(111) terraces in a nearly flat-lying configuration. Through combination of HAS and STM data, we determine that the molecules are bound on step edges with an adsorption energy of about 1.2 eV, which is about 0.2 eV stronger than the adsorption energy we measure on flat surface. Preferential bonding to the under-coordinated Au atoms on step edges suggests that the molecules bind to Au through the nitrogen lone pair. Finally, STM measurements on TMBDA in these two different adsorption configurations show that the highest-occupied molecular orbital is deeper relative to Fermi for the more strongly bound molecules on step edges, confirming that the nitrogen bonds through charge donation to the Au.



INTRODUCTION

Understanding the nature of amine–Au binding is crucial for the advancement of molecular electronics¹ because amine and other nitrogen-based chemical groups have become widely used for binding organic molecules to Au electrodes in single molecule conductance experiments.^{2–6} These linkers are attractive for such measurements because they bind to Au reproducibly, allowing many repeated single-molecule measurements to be performed with consistent outcomes.⁴ Theoretical calculations suggest that amine-terminated molecules bind to under-coordinated Au with a binding energy of about 0.5 eV^{7–9} through the nitrogen lone pair. Thus, they form a relatively weak but selective donor–acceptor bond to an under-coordinated Au atom on the electrode, which allows for reproducible conductance measurements even as the exact geometry of the contact is varied.^{10,11} Other linkers have been found to bind through a similar mechanism, increasing the importance of studying donor–acceptor binding.^{12,13} However, few direct surface studies of amine-terminated molecules on noble metals have been performed to identify their binding structures and electronic properties.^{14–16} Such information could elucidate the mechanism behind the reproducible amine–Au bond and offer clues about other chemical moieties that could be used for single-molecule conductance experiments.

Here we present the first direct observation of the two different binding configurations of 2,3,5,6-tetramethyl-1,4-benzenediamine (TMBDA) on Au and probe their range of binding strengths and

resulting energy-level alignment. We focus on TMBDA as a model system as it has been well characterized in the solid state;¹⁷ electron transport measurements of TMBDA have been carried out by the scanning tunneling microscopy (STM)-based break-junction technique,¹⁸ and TMBDA molecular layers have been studied by X-ray photoemission spectroscopy (XPS) and near-edge X-ray absorption fine structure (NEXAFS) on Au surfaces.¹⁵ In particular, TMBDA has previously been shown to bind to both Au(111) and to under-coordinated Au and to have slightly higher binding energy than the unsubstituted 1,4-benzenediamine on both surfaces.^{15,18} By use of a combination of helium atom scattering (HAS), XPS, low-temperature scanning tunneling microscopy (STM) imaging as well as spectroscopy (STS), we examine the monolayer morphology and electronic properties of TMBDA on Au(111). We show that on flat terraces of the Au(111) surface, the molecules form a packed, ordered monolayer, with the benzene ring lying nearly parallel to the surface. The molecules prefer to adsorb on the hcp and fcc domains,¹⁹ where both nitrogens can coordinate to the Au. We also see that TMBDA exhibits the strongest affinity to under-coordinated atoms at the step edges, consistent with donor–acceptor bonding through the nitrogen. Finally, STS measurements show that this stronger bond

Received: March 17, 2011

Revised: May 17, 2011

Published: May 17, 2011

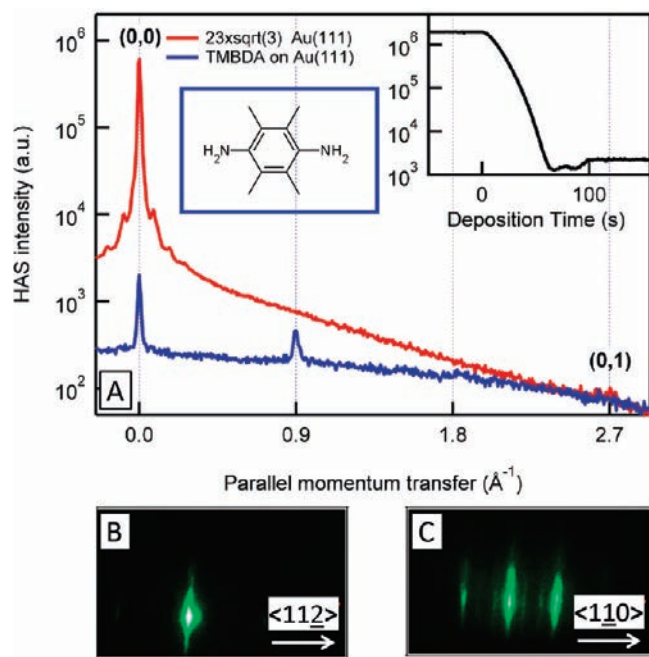


Figure 1. (A) Helium diffraction pattern along $\langle 110 \rangle$ substrate directions for the $(23 \times \sqrt{3})$ -Au(111) chevron reconstruction of the clean surface (red trace) and for the TMBDA monolayer on Au(111) (blue trace). Chemical structure of TMBDA is also shown. Inset: Intensity of the HAS specular peak during deposition as a function of time. (B and C) RHEED along $\langle 112 \rangle$ and $\langle 110 \rangle$ directions, respectively.

on step edges results in the deepening of the molecular HOMO relative to Fermi because of charge donation from the molecule to the Au.¹⁵

EXPERIMENTAL METHODS

HAS and XPS measurements were performed at the ALOISA/HASPES beamline (Elettra Synchrotron, Trieste), and STM measurements were carried out at the Center for Functional Nanomaterials at Brookhaven National Laboratory. TMBDA was purchased from Fluka (>99% purity) and used without further purification. Prior to forming molecular monolayers, the molecule is cleaned by several cycles of pumping at room temperature down to ~ 3 – 6 Torr. Details of monolayer and sub-monolayer preparation in ALOISA/HASPES have been reported elsewhere.¹⁵ For measurements with the STM (Createc LT-STM), a single-crystal Au(111) was first cleaned by two cycles of sputtering with Ar^+ (10^{-5} Torr, 1.5 keV, 10 min) at 25°C and then annealed to temperatures above 400 °C for 10 min in ultrahigh vacuum (UHV). We used a solid Au tip (Alfa Aesar, 99.999% purity), hand cut, and then annealed in UHV. After cleaning, we imaged the sample to confirm that atomically flat surface has been achieved with the characteristic herringbone reconstruction. Subsequently, the sample was brought to room temperature and transferred to the load-lock of the STM which was pumped to a base pressure of 5×10^{-8} Torr. The sample was then exposed to a TMBDA pressure of 5×10^{-6} Torr for 15 min by heating solid molecules to about 40 °C. The sample was transferred back into the STM chamber and cooled to cryogenic temperatures at pressures below 10^{-10} Torr.

RESULTS AND DISCUSSION

A HAS measurement of the surface reflectivity taken during deposition is shown in inset of Figure 1A. HAS specular peak intensity first drops then saturates, consistent with a formation of a saturation phase at room temperature. This phase has previously been attributed to a single monolayer of TMBDA on Au(111).¹⁵ Figure 1A compares HAS diffraction spectra of the clean Au(111) surface with $23 \times \sqrt{3}$ herringbone reconstruction²⁰ and the TMBDA-covered surface which shows additional fractional order peaks along the $\langle 110 \rangle$ direction corresponding to a 3-fold periodicity. Reflection high energy electron diffraction (RHEED) spectra, shown in parts B and C of Figure 1 along the $\langle 110 \rangle$ and $\langle 112 \rangle$ directions, respectively, confirm these findings and indicate no additional periodicity along the latter direction. The narrow shape of specular and fractional HAS diffraction peaks evidence a very high degree of long-range order in the TMBDA covered phase. These measurements indicate that TMBDA monolayers maintain the overall surface structure of the underlying Au(111) and are ordered in the $\langle 110 \rangle$ direction over length scales of hundreds of Ångströms with a 3-fold periodicity.

To investigate the structure of TMBDA films on Au(111) in more detail, we turn to STM, which can serve as a local probe of structural and electronic properties of the molecule on Au. Parts A and B of Figure 2 show STM images of a monolayer of TMBDA on Au(111) taken at 70K. The molecules are roughly hexagonally shaped and about 1 nm in length (Figure 2C) and thus appear to adsorb in a nearly flat-lying configuration on the Au with the plane of the benzene ring parallel to the surface. Despite full coverage, the underlying herringbone reconstruction of Au(111) is clearly visible in Figure 2A,²¹ indicating a relatively weak interaction of amine-terminated molecules with the Au(111) surface.²² In agreement with HAS, all STM images taken reveal the molecules to be well ordered in the $\langle 110 \rangle$ direction with a 3-fold periodicity (Figure 2A). However, there is no additional periodicity along the $\langle 112 \rangle$ direction that is maintained over large areas.

To further investigate the strength of adsorption of our amine-terminated molecules to Au, we image regions of our sample at different coverages by performing temperature dependent desorption studies. We remove our sample from the experimental chamber of the STM and heat it in the preparation chamber where pressure does not exceed about 5×10^{-8} Torr during heating. Previous work has shown that TMBDA on Au(111) starts to desorb at about 70 °C and comes off fully at about 170 °C,¹⁵ but no local-probe investigation into relative binding strengths of adsorption geometries have been performed. Parts A and B of Figure 3 show STM images of sub-monolayers created by flashing the saturated monolayer to 100 and 120 °C, respectively. About a third of the monolayer is lost by heating the sample to 100 °C as estimated from STM images (Figure 3A), but even on the Au(111) terraces, molecules do not come off evenly from all parts of the surface; flashing leaves clear empty Au(111) regions. These empty regions coincide with the discommensuration (bright) lines of the herringbone reconstruction, where the hexagonal close-packed (hcp) and face-centered cubic (fcc) regions of Au(111) surface merge.¹⁹ Further flashing to higher temperatures brings the coverage on flat terraces even lower, with few remaining molecules clustering in groups of three or four on the hcp and fcc regions as shown in Figure 3B. These groupings could be a result of weak hydrogen bonding previously reported for this molecule.¹⁷ Strikingly, after a flash to 120 °C, the step edges remain fully decorated with molecules even while

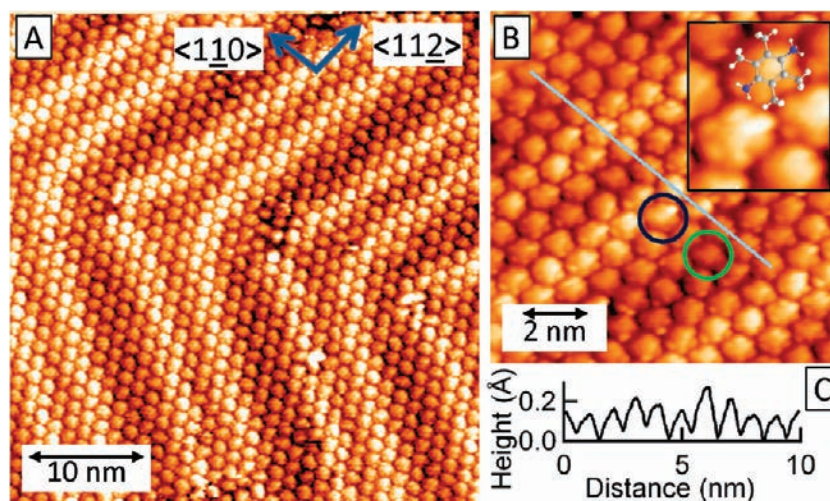


Figure 2. (A) STM images taken at 70 K of the saturated TMBDA monolayer with +165 mV bias applied to the substrate and 130 pA set-point current. (B) Smaller scale image of the same area as shown in A taken in the same tunnelling conditions. Inset shows chemical structure superimposed on the high resolution STM image of TMBDA. (C) The profile along the $\langle 110 \rangle$ line indicated in B.

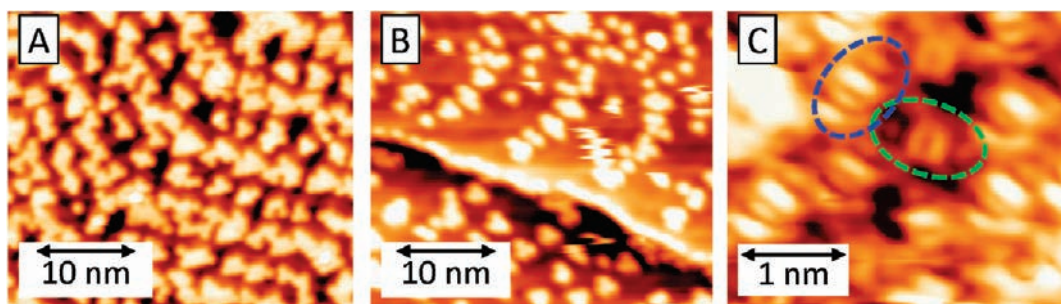


Figure 3. (A) A flat terrace at 5 K after flashing to 100 °C, imaged at +100 mV bias applied to the sample, with set-point current of 150 pA. (B) Terrace and step edge at 5 K after flashing to 120 °C, imaged at +100 mV bias applied to the substrate, with set-point current of 75 pA. (C) An image of the area between two herringbone lines (top left corner and bottom right corner) taken on a different part of the sample at −295 mV sample bias at set-point current of 200 pA. An example of an elongated molecule is circled in blue and a symmetrical molecule is circled in green.

the flat terraces are nearly empty (Figure 3B). We can combine our new findings with previous results¹⁵ to estimate the adsorption energy of molecules on flat surface and on step edges. Knowing that molecules on flat Au desorb at about 100 °C and molecules on step edges desorb at about 170 °C, we can determine approximate adsorption energies. We use the desorption measurements from our previous work,¹⁵ where we monitored the HAS specular peak while heating the substrate at a 5 K/s rate. By application of the Redhead formula²³ and using standard parameters for first-order desorption kinetics for conjugated molecules,²⁴ we find adsorption energies of 1 eV on the flat surface and around 1.2 eV on the step edges. We note here that these adsorption energies are higher than those computed with density functional theory (DFT) possibly due to a lack of van der Waals interactions in standard DFT.^{7,8,25,26}

We now investigate the origin of uneven desorption off Au(111) terraces upon flashing. As already discussed, desorption studies show that molecules attached along the bright lines of the herringbone are bound more weakly than molecules on the darker regions of the reconstruction. Indeed, closer inspection of Figure 2B reveals that the more strongly bound molecules found predominantly on the hcp and fcc regions of the surface appear

more symmetric (blue circles) than the more weakly bound counterparts along the herringbone (green circles) in the full monolayer. A zoomed-in image in Figure 3C shows the difference between two species with higher resolution where molecules on the herringbone appear tilted (circled in green), whereas molecules between herringbone lines are more symmetrically bound (circled in blue). This suggests that the flat molecules are bound with both nitrogens equally coordinated to the surface. In contrast, the weaker bound molecules on the flat Au surface which appear tilted, are probably bound through only one nitrogen and desorb from the surface first.

To investigate the nature of the distinct binding configurations of TMBDA on flat Au(111) we perform carbon and nitrogen XPS, which is known to be sensitive to the chemical environment of atomic species in the molecule and their distance from the metal surface.^{27,28} XPS can thus distinguish different binding chemistries of the two distinct molecular species identified in the STM images. For reference, we first performed XPS of a multilayer of our molecules on Au(111). Our multilayers are estimated to be over 2 nm thick, so the influence of the substrate on electron energy is negligible. Figure 4A shows two distinct C1s core-electron binding energies of the multilayer at 284.4 and 285.1 eV which can

be assigned from the literature to the distinct chemical environments for carbon TMBDA—the substituent methyl groups and the benzene ring respectively.²⁹ The carbons closest to the amines should display a slight shift in the core–electron binding energy with respect to the other carbons in the benzene ring, but this shift is too small to resolve. The ratio of the area under the two carbon XPS peaks is 0.6 and agrees well with the 4:6 ratio of methyl groups to aromatic carbons. Only one species of nitrogen is present in the multilayer (Figure 4B), identified by a core–electron binding energy of 399.2 eV. This indicates that in the multilayer, the two ends of the molecule are identical and any hydrogen bonding differences between the two ends in the solid state induce shifts that are not resolved here.¹⁷

In Figure 4, we show also XPS spectra measured on a saturated monolayer of TMBDA on Au(111), prepared as described above. We see that the C1s peaks are shifted to lower binding energy by about 0.7 eV, due to the electrostatic screening effects when TMBDA is in close proximity to the Au surface.^{28,30} However, a small fraction of the signal (about 1/10th) remains at 285.2 eV, at the same binding energy as the benzene ring C in the multilayer.

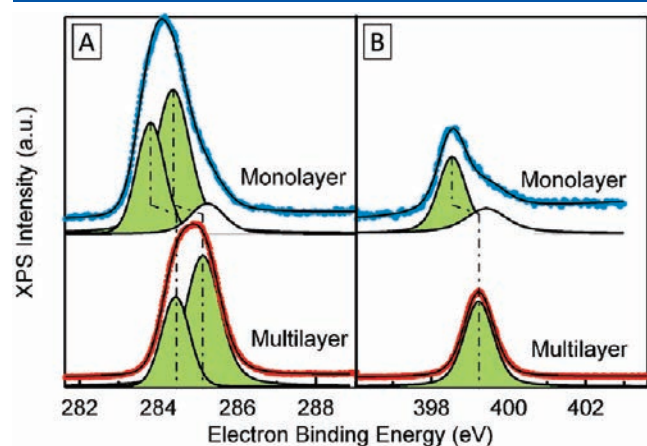


Figure 4. (A and B) XPS on carbon and nitrogen, respectively, performed using a photon energy of 500 eV. For both species, spectra for the monolayer and multilayer coverage are shown. The multilayer signal was scaled by 0.15 for comparison with the monolayer. Traces are offset vertically for clarity.

Similarly, most of the N1s XPS signal shifts down in energy by about 0.7 eV, though a small signal (about 1/3rd) is visible at the same energy as the N1s peak seen for the multilayer film. Since molecules are weakly bound on Au(111), the shifts seen here are most likely due to electrostatic effects rather than chemical interaction. We thus conclude that about 1 in 11 carbon atoms and 1 in 4 nitrogen atoms are far from the surface, indicating that about half the molecules are in a slightly tilted geometry with only one N coordinating the gold. This is consistent with the STM image in Figure 3A, which shows a similar prevalence of both flat and tilted species.

To further examine the nature of this nitrogen bond to Au and to investigate the effect of a reduced Au coordination played in molecular adsorption on step edges, we perform STS measurements on TMBDA on Au(111) at 5 K. Parts A and B of Figure 5 show the area used for STS measurements where molecules bound on the terrace and along a step edge are present. Furthermore, the zoomed in image of the step edge shown in the inset of Figure 5B emphasizes the changed electronic structure of molecules bound there with respect to those bound on flat terraces, pointing to the effect of stronger binding to undercoordinated atoms on the electronic structure of TMBDA. Figure 5C shows an average of at least 40 current–voltage (*I*(*V*)) and differential conductance (*dI/dV*) curves taken on edge (green traces) and terrace-bound (blue traces) TMBDA at the locations indicated in Figure 5B. Because of the weak Au–N bond, we were not able to use integration times higher than 2 s per voltage ramp without desorbing molecules during the measurement. To compensate for the short integration time and ensure that surface was not altered by the measurement, we took many fast *I*(*V*) ramps and averaged at least 40 consecutive spectra, imaging the surface after a series of *I*(*V*) measurements to ensure that the coverage had not changed. To obtain *dI/dV* representing the local electronic density of states (LDOS) on the substrate³¹ we used a 40 mV oscillation at a frequency of 2kHz and lock-in detection of the first harmonic. We see, in Figure 5C, steeper increase in current in the *I*(*V*) spectra and a greater LDOS in the filled part of the spectrum for terrace-bound TMBDA when compared with the edge-bound molecules. A clear peak, indicating the position of the HOMO for edge-bound TMBDA, is seen at -1.7 eV. In contrast, we do not see a clear single Lorentzian peak for the terrace-bound TMBDA. It is likely

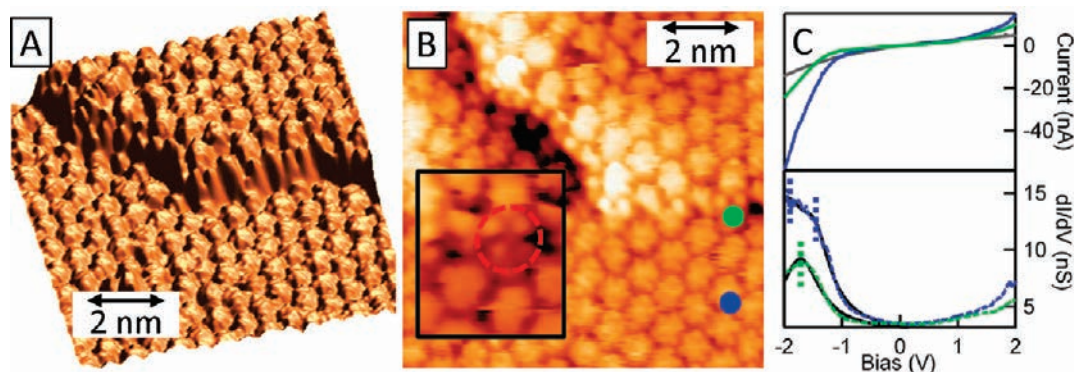


Figure 5. (A and B) A 3D rendering and 2D image of a full monolayer of molecules on flat terraces and on the edge taken with +65 mV tunneling bias and 90 pA set point current. Inset to B shows a smaller scale image of the molecules bound on the edge, circled in red. (C) STS spectra (*I*–*V* shown on the top panel, and *dI/dV* shown on the bottom panel) taken on B with the same tunneling parameters on step edge and on terrace (green and blue spots) and on clean gold (gray). Each trace is an average of at least 40 individual spectra, each taken over 2 s using lock-in techniques. *dI/dV* spectra are fit with Lorentzian peaks, where the green displays a single peak within the range probed at -1.7 V (dashed green line). The blue is best fit with two Lorentzians, centered at -1.5 and -2.0 V (dashed blue lines).

that for these terrace-bound molecules, both HOMO and HOMO-1 are closer to Fermi, resulting in a wide feature in the dI/dV spectrum. We fit this wide peak with a double Lorentzians and find two peaks at -1.5 and -2.0 eV which we attribute to the highest-occupied molecular orbital (HOMO) and HOMO-1, respectively. Using these results, we conclude that the HOMO shifts away from Fermi in TMBDA bound on under-coordinated Au, in excellent agreement with previous photoemission studies.¹⁵ Clearly, the stronger binding of the molecules on step-edges results in a lowering of the occupied molecular orbitals relative to Fermi, indicating that the N-lone pair donates charge to under-coordinated Au. The tops of under-coordinated step-edges are known to be electron poor and therefore can act as good acceptors for the N-lone pair on the TMBDA.³² Finally, the unoccupied side of the STS spectra do not show any features or resonances within 2 eV of Fermi, confirming that the HOMO constitutes the dominant conductance channel in single molecule transport measurements.

CONCLUSIONS

We determine, using HAS, STM, and XPS measurements, the structure of TMBDA monolayers on Au(111). XPS and STM reveal that about half of the molecules on Au(111) terraces are lying flat with both nitrogens coordinating to Au atoms on the surface, while the remaining are slightly tilted, with one unbound nitrogen. HAS temperature desorption studies combined with STM images show that molecules adsorb on step edges with an adsorption energy that is higher than on Au(111) terraces. Finally, STS shows that this stronger Au–N bond results in greater charge transfer to the Au, as evidenced by the deepening of the molecular HOMO on molecules bound to under-coordinated Au atoms on step edges.

AUTHOR INFORMATION

Corresponding Author

*E-mail: morgante@tasc.infn.it (A.M.); lv2117@columbia.edu (L.V.).

ACKNOWLEDGMENT

We gratefully acknowledge Prof. Sylvio Modesti, Dr. Peter Sutter, and Dr. Mark S. Hybertsen for discussion of STM and STS techniques and the experimental results. This work was supported in part by the NSEC program of the NSF (Grant CHE-0641523), and by the Packard Foundation. It was also supported through MiUR-PRIN2008-prot.20087NX9Y7_002. Portions of this work were performed at the Center for Functional Nanomaterials, Brookhaven National Laboratory, and were supported by the Office of Science, Office of Basic Energy Sciences, of the U.S. Department of Energy.

REFERENCES

- (1) Aviram, A.; Ratner, M. A. Molecular Rectifiers. *Chem. Phys. Lett.* **1974**, *29*, 277–283.
- (2) Mishchenko, A.; Vonlanthen, D.; Meded, V.; Burkle, M.; Li, C.; Pobelov, I. V.; Bagrets, A.; Viljas, J. K.; Pauly, F.; Evers, F. Influence of Conformation on Conductance of Biphenyl-Dithiol Single-Molecule Contacts. *Nano Lett.* **2010**, *10*, 156–163.
- (3) Kiguchi, M.; Miura, S.; Takahashi, T.; Hara, K.; Sawamura, M.; Murakoshi, K. Conductance of Single 1,4-Benzenediamine Molecule Bridging between Au and Pt Electrodes. *J. Phys. Chem. C* **2008**, *112*, 13349–13352.

- (4) Venkataraman, L.; Klare, J. E.; Tam, I. W.; Nuckolls, C.; Hybertsen, M. S.; Steigerwald, M. L. Single-Molecule Circuits with Well-Defined Molecular Conductance. *Nano Lett.* **2006**, *6*, 458–462.
- (5) Xu, B. Q.; Tao, N. J. J. Measurement of Single-Molecule Resistance by Repeated Formation of Molecular Junctions. *Science* **2003**, *301*, 1221–1223.
- (6) Wu, S. M.; Gonzalez, M. T.; Huber, R.; Grunder, S.; Mayor, M.; Schonberger, C.; Calame, M. Molecular Junctions Based on Aromatic Coupling. *Nat. Nano.* **2008**, *3*, 569–574.
- (7) Hybertsen, M. S.; Venkataraman, L.; Klare, J. E.; Whalley, A. C.; Steigerwald, M. L.; Nuckolls, C. Amine-Linked Single-Molecule Circuits: Systematic Trends across Molecular Families. *J. Phys.: Cond. Mat.* **2008**, *20*, 374115.
- (8) Hoff, R. C.; Ford, M. J.; McDonagh, A. M.; Cortie, M. B. Adsorption of Amine Compounds on the Au(111) Surface: A Density Functional Study. *J. Phys. Chem. C* **2007**, *111*, 13886–13891.
- (9) Frei, M.; Aradhya, S. V.; Koentopp, M.; Hybertsen, M. S.; Venkataraman, L. Mechanics and Chemistry: Single Molecule Bond Rupture Forces Correlate with Molecular Backbone Structure. *Nano Lett.* **2011**, *11*, 1518–1523.
- (10) Li, Z.; Kosov, D. S. Nature of Well-Defined Conductance of Amine Anchored Molecular Junctions. *Phys. Rev. B* **2007**, *76*, 035415.
- (11) Kamenetska, M.; Koentopp, M.; Whalley, A.; Park, Y. S.; Steigerwald, M.; Nuckolls, C.; Hybertsen, M.; Venkataraman, L. Formation and Evolution of Single-Molecule Junctions. *Phys. Rev. Lett.* **2009**, *102*, 126803.
- (12) Park, Y. S.; Whalley, A. C.; Kamenetska, M.; Steigerwald, M. L.; Hybertsen, M. S.; Nuckolls, C.; Venkataraman, L. Contact Chemistry and Single-Molecule Conductance: A Comparison of Phosphines, Methyl Sulfides, and Amines. *J. Am. Chem. Soc.* **2007**, *129*, 15768–15769.
- (13) Bagrets, A.; Arnold, A.; Evers, F. Conduction Properties of Bipyridinium-Functionalized Molecular Wires. *J. Am. Chem. Soc.* **2008**, *130*, 9013–9018.
- (14) Wang, W. H.; Shi, X. Q.; Lin, C. S.; Zhang, R. Q.; Minot, C.; Van Hove, M. A.; Hong, Y. N.; Tang, B. Z.; Lin, N. Manipulating Localized Molecular Orbitals by Single-Atom Contacts. *Phys. Rev. Lett.* **2010**, *105*, 126801.
- (15) Dell'Angela, M.; Kladnik, G.; Cossaro, A.; Verdini, A.; Kamenetska, M.; Tamblyn, I.; Quek, S. Y.; Neaton, J. B.; Cvetko, D.; Morgante, A. Relating Energy Level Alignment and Amine-Linked Single Molecule Junction Conductance. *Nano Lett.* **2010**, *10*, 2470–2474.
- (16) Martin, C. A.; Ding, D.; van der Zant, H. S. J.; van Ruitenbeek, J. M. Lithographic Mechanical Break Junctions for Single-Molecule Measurements in Vacuum: Possibilities and Limitations. *New J. Phys.* **2008**, *10*, 065008.
- (17) Sobczyk, L.; Prager, M.; Sawka-Dobrowolska, W.; Bator, G.; Pawlukojc, A.; Grech, E.; van Eijck, L.; Ivanov, A.; Rols, S.; Wuttke, J.; et al. The Structure of Diaminodurene and the Dynamics of the Methyl Groups. *J. Chem. Phys.* **2009**, *130*, 164519.
- (18) Venkataraman, L.; Park, Y. S.; Whalley, A. C.; Nuckolls, C.; Hybertsen, M. S.; Steigerwald, M. L. Electronics and Chemistry: Varying Single Molecule Junction Conductance Using Chemical Substituents. *Nano Lett.* **2007**, *7*, 502–506.
- (19) Barth, J. V.; Brune, H.; Ertl, G.; Behm, R. J. Scanning Tunneling Microscopy Observations on the Reconstructed Au(111) Surface - Atomic-Structure, Long-Range Superstructure, Rotational Domains, and Surface-Defects. *Phys. Rev. B* **1990**, *42*, 9307–9318.
- (20) Harten, U.; Lahee, A. M.; Toennies, J. P.; Woll, C. Observation of a Soliton Reconstruction of Au(111) by High-Resolution Helium-Atom Diffraction. *Phys. Rev. Lett.* **1985**, *54*, 2619–2622.
- (21) Woll, C.; Chiang, S.; Wilson, R. J.; Lippel, P. H. Determination of Atom Positions at Stacking-Fault Dislocations on Au(111) by Scanning Tunneling Microscopy. *Phys. Rev. B* **1989**, *39*, 7988–7991.
- (22) Silly, F.; Shaw, A. Q.; Castell, M. R.; Briggs, G. A. D.; Mura, M.; Martsinovich, N.; Kantorovich, L. Melamine Structures on the Au(111) Surface. *J. Phys. Chem. C* **2008**, *112*, 11476–11480.
- (23) Redhead, P. A. Thermal Desorption of Gases. *Vacuum* **1962**, *12*, 203–211.

- (24) Fichthorn, K. A.; Miron, R. A. Thermal Desorption of Large Molecules from Solid Surfaces. *Phys. Rev. Lett.* **2002**, *89*, 196103.
- (25) Bilic, A.; Reimers, J. R.; Hush, N. S.; Hafner, J. Adsorption of Ammonia on the Gold(111) Surface. *J. Chem. Phys.* **2002**, *116*, 8981–8987.
- (26) Dion, M.; Rydberg, H.; Schroder, E.; Langreth, D. C.; Lundqvist, B. I. Van Der Waals Density Functional for General Geometries. *Phys. Rev. Lett.* **2004**, *92*, 246401.
- (27) Hufner, S.; Schmidt, S.; Reinert, F. Photoelectron Spectroscopy - an Overview advanced Materials. *Nucl. Instrum. Meth. A* **2005**, *547*, 8–23.
- (28) Bjorneholm, O.; Tillborg, H.; Nilsson, A.; Martensson, N.; Agren, H.; Liegener, C. M. Vibrationally and Orientationally Selective Probing of Intramolecular Potentials in Physisorbed Molecules. *Phys. Rev. Lett.* **1994**, *73*, 2551–2554.
- (29) Ohta, T.; Fujikawa, T.; Kuroda, H. Core-Electron Spectra of Monosubstituted Benzenes Obtained by Gas-Phase X-Ray Photoelectron-Spectroscopy. *B. Chem. Soc. Jpn.* **1975**, *48*, 2017–2024.
- (30) Ishii, H.; Sugiyama, K.; Ito, E.; Seki, K. Energy Level Alignment and Interfacial Electronic Structures at Organic Metal and Organic Organic Interfaces. *Adv. Mater.* **1999**, *11*, 605–625.
- (31) Stroscio, J. A.; Kaiser, W. J. *Scanning Tunneling Microscopy*; Academic Press, San Diego, CA, 1993.
- (32) Smoluchowski, R. Anisotropy of the Electronic Work Function of Metals. *Phys. Rev.* **1941**, *60*, 661.